GMR
The Original

Association of UAV-based vegetation indices with soybean yield and disease severity

NJD Vilela[1], MAJ. Ferraz[1]*, AT Bruzi[1], GLD. Vilela[1] and GAS Ferraz[2]

[1]Department of Agriculture, Universidade Federal de Lavras, Lavras, MG, Brazil.
[2]Department of Agricultural Engineering, Universidade Federal de Lavras, Lavras, MG, Brazil.

Corresponding author: Marcelo Araújo Junqueira Ferraz
E-mail: marcelo.ferraz1@estudante.ufla.br

Genet. Mol. Res. 23 (3): gmr2380
Received September 12, 2024
Accepted September 18, 2024
Published September 23, 2024
DOI http://dx.doi.org/10.4238/gmr2380

ABSTRACT. Red–green–blue (RGB) and multispectral remote sensing sensors onboard unmanned aerial vehicles (UAVs), which are nondestructive, economical and flexible tools, have been widely adopted in crop monitoring and management, especially for efficient monitoring and identification of foliar diseases in soybean crops. The objective of this study was to establish correlations between vegetation indices obtained by UAVs and the yield grain and Asian soybean rust and powdery mildew severity in soybean crops under tropical conditions. Six commercial soybean cultivars with INOX® technology (TMG 7060 IPRO, TMG 7063 IPRO, TMG 7262 RR, TMG 7062 IPRO, TMG 7363 RR, and TMG 7067 IPRO), one multiline cultivar (a mixture of lines) and one susceptible control cultivar for Asian soybean rust and powdery mildew (M6410 IPRO) were evaluated. The experiments were performed in Lavras, Ijaci and Nazareno in the state of Minas Gerais during the 2020/21 season. The experimental design encompassed randomized complete blocks, with treatments split into subdivided bands (four fungicide application treatments and seven cultivar treatments + one multiline treatment) in three replications. The fungicide applications were assigned to the main plots, while the cultivars were assigned to the subplots. Aerial images were collected by a DJI Mavic Pro equipped with an RGB sensor and a DJI Matrice 100 equipped with a Parrot Sequoia multispectral sensor. The traits evaluated included Asian soybean rust severity, powdery mildew severity, defoliation index, grain yield,

normalized difference vegetation index (NDVI) and modified chlorophyll uptake ratio index (MPRI). Joint analyses (multienvironment) and analyses of the subdivided plots over time were conducted. The NDVI (ρ = 0,62) and MPRI (ρ = 0,76) exhibited significant correlations, facilitating the use of RGB and multispectral imaging in high-throughput phenotyping to assess the soybean grain yield in high-altitude tropical climates. Like the variable disease severity, whose NDVI and MPRI indices showed a correlation with the severity of Asian rust (ρ = - 0.95) and powdery mildew (ρ = -0.47), respectively.

Key words: Aerial images; Genotype × Environment interaction; *Erysiphe difusa; Phakopsora pachyrhizi*; Multispectral images.

INTRODUCTION

Soybean [*Glycine max* (L.) Merril] is the fourth leading cultivated crop globally and the most-traded agricultural commodity, representing approximately nine percent of the total agricultural trade value (Shammi et al., 2024). However, foliar disease epidemics can cause substantial economic losses in agricultural environments and undermine the sustainability of agricultural operations.

Diseases can be recognized based on traditional methods, which are often subjective, strictly dependent on the observer, time consuming and prone to inaccuracies and ambiguities. Proper detection techniques and reliable diagnostic methods for disease identification are essential for saving time and minimizing crop damage (Abbas et al., 2023). The continued adoption of recent advanced technologies, such as smart algorithms and sophisticated sensors onboard unmanned aerial vehicles (UAVs), is revolutionizing agricultural crop monitoring.

UAV-based remote sensing enables the rapid observation and screening of crop diseases on a large scale in an objective and nondestructive manner. Currently, aerial images within the visible spectrum (red–green–blue, RGB) and multispectral images are available from different sensors onboard UAVs, mainly due to their notable flight flexibility (Shahi et al., 2023).

Vegetation indices (VIs) allow the evaluation and observation of changes in the biophysical properties of the canopy, such as the leaf area index, chlorophyll content and photosynthetically active radiation. In turn, biophysical properties are influenced by the presence of diseases, which may explain why the severity is significantly correlated with the VI values for crops (Zhao et al., 2020). In a few studies, the successful application of disease estimation using UAV-based remote sensing has been reported (Shahi et al., 2023).

In many studies on plant phenotyping, RGB (Alves et al., 2021) and multispectral (Shammi et al., 2024) sensors incorporated into UAVs, RGB image fusion and deep learning for disease identification (Bevers; Sikora; Hardy, 2022) and the application of vegetation indices for predicting the grain yield (Silva et al., 2020) have been employed. High-throughput phenotyping has yielded an increase in the efficiency of crop genetic improvement (Moreira et al., 2021).

Therefore, the objective of this study was to investigate the associations of vegetation indices based on UAV-obtained RGB and multispectral images with the Asian soybean rust and powdery mildew severity and yield grain of soybean crops under tropical conditions.

MATERIALS AND METHODS

The experiments were conducted during the 2017/2018 and 2018/2019 crop season. In the first year, experiments were conducted in two locations, Lavras and Ijaci, in the Minas Gerais state (MG). In the second year, experiments were carried out in four locations in MG (Lavras, Ijaci, Itutinga, and Inconfidentes). In each year, the experiments were sown within the same time period. Four experiments were conducted each year and in each location; thus, in combining the total number of sites and experiments, we have eight environments (2 locations × 4 experiments) in the first year and 16 environments (4 locations × 4 experiments) in the second year, for a total of 24 environments.

Study area

The experiments were conducted in three environments during the 2020/2021 agricultural season, namely, (a) the Technology Development and Transfer Center of the Federal University of Lavras in Ijaci, Minas Gerais, Brazil, with an average altitude of 845 m (21° 9'51.94" S, 44°55'6.17" W); (b) the Center for Scientific and Technological Development in Agriculture (Muquém Farm) of the Federal University of Lavras, Lavras, Minas Gerais, Brazil, with an average altitude of 950 m (21°12'11" S, 44°58'47" W); and (c) Science, Technology, and Engineering at Rehagro Search, Nazareno, Minas Gerais, Brazil, with an altitude of 1003 m (21°15'32" S, 44°30'56" W). The experimental region is subject to the Cwa climate classification (Figure S1), characterized as a subtropical climate with dry winters and hot summers (Köppen, 1948).

Genetic treatments and experimental process

The experiment was conducted in a no-tillage system, with seed furrows spaced at 0.50 m. Six soybean cultivars with INOX® technology, one multiline cultivar, which indicates a mixture of genotypes with relatively high population homeostasis, and one susceptible cultivar were applied (Table S1). For multiline sowing, three seeds of each INOX® cultivar were mixed, totaling 18 seeds per linear meter.

The experimental design was a randomized complete block design (RCBD), with treatments divided into split-plot strips, totaling 4 × 8 treatments (four fungicide application management treatments and seven cultivar treatments + one multiline treatment) in three replications. The fungicide applications were assigned to the plots, and the cultivars were assigned to the subplots (Table 1).

The plots exhibited dimensions of 4 m × 0.5 m with a row spacing of 0.5 m and 18 seeds per meter. The two central rows were considered useful areas for the plots. Manual sowing was performed in a no-tillage system during the first half of December 2020, and harvesting was performed in March 2021. Inoculation via furrows was conducted after sowing with E. japonicum

Table 1. Number of fungicide applications used and stages of soybean plant development.

Number of applications	Phenological stage of applications
0	Control
1	R1*
2	R1 e R1 + 15**
3	R1, R1 + 15** e R1 + 30**

*Flowering time, ** Days after R_1.

of seed strains SEMIA 5079 and 5080 at a rate of 18 mL a.i. kg-1, which contained 10.8 × 106 CFU/ seed of Nitragin Cell Tech HC® inoculant (3x109 CFU.mL^{-1}).

For application purposes, a motorized backpack sprayer equipped with a bar and four XR 11002 spray nozzles was employed, and a spray volume equivalent to 150 L ha^{-1} was applied. Crop pest control was performed as needed using neonicotinoids, pyrethroids, and chlorpyrifos. Postemergence weed control was conducted using glyphosate at a dosage of 2 L ha^{-1}. Only fungicide Fox Xpro® (trifloxystrobin; prothioconazole, bixafen) was applied at the recommended dosage of 0.4 L a.i. ha^{-1}. For application purposes, a motorized backpack sprayer equipped with a bar and four XR 11002 spray nozzles spaced 50 cm apart was used, which was calibrated for a flow rate of 150 L ha^{-1}. The recommended adjuvant was added to the fungicide at the manufacturer-recommended dosage at the time of application.

Genetic treatments and experimental process

The severity of Asian soybean rust (*Phakopsora pachyrhizi*) was quantified by assessing the percentage of the leaf area covered with disease symptoms using a diagrammatic scale (Figure S2a), which was developed by Godoy, Koga and Canteri (2006). For powdery mildew (*Erysiphe diffusa*), a diagrammatic scale (Figure S2b) developed by Mattiazzi (2003) was adopted.

Three trifoliate leaves per plant were evaluated, one from the upper third, one from the middle third, and one from the lower third. This yielded a total of nine leaflets evaluated per plot, and the average severity is an estimate of the mean disease severity in the plot.

Defoliation in the plots was evaluated by a single evaluator based on the diagrammatic scale developed by Hirano et al., (2010). This scale provides visual reference points for assessing the extent of leaf loss or defoliation in plants. By comparing the observed defoliation with the reference images of the diagrammatic scale, the defoliation level in each plot was estimated. Data collection involved evaluating the grain yield, which was determined by plot harvesting. After standardizing the grain moisture to 13%, the yield was estimated in kg ha^{-1} by converting the area of each plot.

Image acquisition and processing

Images were captured using a Phantom 4 UAV (SZ DJI Technology Co., Shenzhen, China) equipped with an RGB camera (model FC330, DJI, Shenzhen, China) and a Matrice 100 UAV (SZ DJI Technology Co., Shenzhen, China) equipped with a Parrot Sequoia multispectral sensor (Parrot Drones SAS, Paris, France). The Sequoia sensor allows data collection within four spectral bands: green (550 nm), red (660 nm), red edge (735 nm) and near infrared (NIR 790 nm). The images from these four bands exhibit a resolution of 1.2 megapixels and a radiometric resolution of 16 bits.

The UAV flights were synchronized with field phenotypic assessments and executed from 10:00 am to 1:00 pm. All flight missions were performed at an altitude of 40 m with an approximate speed of 5 m.s^{-1}. The images exhibited a ground sampling distance (GSD) of 0.85 cm per pixel, incorporating 80% frontal overlap and 70% side overlap. Flight routes were automatically generated using Pix4D Capture software (version 4.13.1, Pix4d SA, Prilly, Switzerland).

Four ground control points (GCPs) were strategically positioned within the study area to ensure precise geographic referencing of the acquired images. The geographic coordinates of these points were obtained using GPS equipment, with a Spectra SP60 receiver (Spectra Geospatial, Trimble Inc., Sunnyvale, United States) operating in real-time kinematic (RTK) mode.

Notably, multispectral images were collected on March 10 and 23, 2021, corresponding to phenological stages R5 and R7, respectively. Then, the images were processed using Photoscan Professional software (version 1.2.4, Agisoft LLC, St. Petersburg, Russia), which involves a systematic workflow that encompasses image alignment, dense point cloud generation and orthomosaic development for each assessment date. Phenotypic assessments were conducted in the field. Moreover, vegetation indices were derived from Parrot sensor-acquired multispatial images using QGIS software (version 3.16.1, QGIS Development Team, Trondheim, Norway). The orthomosaic ground and vegetation portions were segmented through a supervised classification approach using the Dzetsaka Classification Tool plugin within QGIS software.

To minimize edge effects on plant reflectance, a negative buffer of 0.5 m was applied within each parcel. The selection of vegetation indices (Table 2) was motivated by their established correlation with key biophysical traits of crops, including biomass, canopy health, and chlorophyll content (Ferraz et al., 2024).

Table 2. Vegetation indices for multispectral images from the Parrot sensor.

Vegetation index	Equation	Reference
NDVI	$\frac{(NIR - Red)}{(NIR + Red)}$	(Rouse et al., 1974)
MPRI	$\frac{(Green - Red)}{(Green + Red)}$	(Yang; Willis; Mueller, 2008)

NDVI: Normalized Difference Vegetation Index; MPRI: Modified Photochemical Reflectance Index.

Statistical analysis of phenotypic data

The experiments at each location were individually analyzed by Model one, considering all response variables to evaluate the residue normality based on the Shapiro–Wilk test (Shapiro; Wilk, 1965) and to detect variance homogeneity using the maximum F test (Hartley, 1950), according to the model:

$$y_{ij} = \mu + \beta_j + \theta_i + e_{ij} \quad (1)$$

where y_{ij} is the value for the trait analyzed in genotype i in block k for site j; μ is the constant associated with all observations, assumed to be fixed; β_j is the effect of block j, assumed to be fixed; θ_i is the effect of genotype i, assumed to be fixed; and e_{ij} is the effect of the error associated with the observation of genotype i in block j, assumed to be random ($e_{ij} \sim$ N (0, $\sigma^2_{e_{ij}}$)).

After the residual variance homogeneity test, a joint analysis of the environments was performed to estimate the best linear unbiased estimators (BLUEs) using a mixed model approach. Additionally, two partitioning analyses were conducted, one between the effects of two regular treatments (which feature INOX technology) and another between the multiline and susceptible control cultivar treatments.

Contrasts were made between the regular treatment effect and the overall mean, as well as between the regular treatment effect and the control treatment, for the evaluated variables. For variables where the assumption of variance homogeneity was not met, a diagonal variance matrix structure $e_{ik} \sim N(0, \bigoplus_{j=1}^{j} I\sigma^2_e)$ was adopted, according to the model (Barbosa, 2009; Henderson, 1975).

$$\bar{y} = \mu + X_l u_l + X_r u_r + X_a \tau_a + X_g \tau_g + X_{ga} \tau_{ga} + X_{gl} u_{gl} + X_{la} u_{la} + \varepsilon \quad (2)$$

where ȳ represents the observed value for the analyzed characteristic; μ is the constant associated with all observations; $X_l u_l$: vector of random local effects, assuming that $l \sim N(0, \sigma_l^2)$; $X_r u_r$ is the vector of random within-local replication effects, $g \sim N(0, \sigma_r^2)$; $X_a \tau_a$ is the vector of fixed application effects; $X_g \tau_g$ is the vector of fixed cultivars effects; $X_{ga} \tau_{ga}$ is the vector of fixed treatment-application interaction effects; $X_{gl} u_{gl}$ is the vector of random treatment-local interaction effects, $gl \sim N(0, \sigma_{gl}^2)$; $X_{la} u_{la}$ is the vector of random local-application interaction effects, $la \sim N(0, \sigma_{la}^2)$; and ε is the vector of associated error effects (random), $\varepsilon \sim N(0, I\sigma_\varepsilon^2)$.

The Asian rust area under the disease progress curve (AUDPC) was obtained by:

$$AUDPC = \sum_{i=1}^{n} \left[\frac{Y_{i+1} + Y_i}{2} x (T_{j+1} - T_j) \right] \quad (3)$$

where *AUDPC* is the area under the disease progress curve; Y_i is disease severity at the time of evaluation i; Y_{i+1} is disease severity at the time of evaluation i+1; T_j is the time of evaluation j, in number of days; and T_{j+1} is the time of evaluation j+1. The data collected from the middle, upper, and lower thirds of the plants in each plot were subjected to model three, which corresponds to the nested analysis:

$$\bar{y} = \mu + X_l u_l + X_r u_r + X_a \tau_a + X_g \tau_g + X_{ga} \tau_{ga} + X_{gl} u_{gl} + X_p u_p + X_{la} u_{la} + \varepsilon \quad (4)$$

where ȳ is the observed value for the analyzed characteristic; μ is the constant associated with all observations; $X_l u_l$ is the vector of random local effects, assuming that $l \sim N(0, \sigma_l^2)$; $X_r u_r$: vector of random within-local replication effects, $g \sim N(0, \sigma_r^2)$; $X_a \tau_a$ is the vector of fixed application effects; $X_g \tau_g$ is the vector of fixed treatment effects; $X_{ga} \tau_{ga}$ is the vector of fixed treatment-application interaction effects; $X_{gl} u_{gl}$ is the vector of random treatment-local interaction effects, $gl \sim N(0, \sigma_{gl}^2)$; $X_p u_p$ is the vector of random position effects aligned with treatments, $p \sim N(0, \sigma_p^2)$; $X_{la} u_{la}$ is the vector of random local-application interaction effects, $la \sim N(0, \sigma_{la}^2)$; ε is the vector of associated error effects (random), $\varepsilon \sim N(0, I\sigma_\varepsilon^2)$.

The vegetation indices were analyzed using a model following a repeated measures design over time. This approach was used to account for the effect of collecting repeated measures within the same plot and to obtain an adjusted mean value for the different indices to represent the plot-level response. In the analysis procedure, the repetitions were adjusted based on the combination of replication, location, and application effects, resulting in a total of 36 repetitions.

The experimental precision was evaluated using the average accuracy ($r\hat{g}g$) according to Resende; Silva and Azevedo (2014), as estimated by the equation:

$$r\hat{g}g = \sqrt{1 - \frac{1}{F_g}} \quad (5)$$

Pearson's correlation correlation (ρ) was calculated using the fitted values between the different analysis variables to assess the association between the experimental variables and the results obtained from the vegetation indices. The significance of the correlations was assessed using the t test at significance levels of 0.05 and 0.2. The R environment (version 4.1.3, R Core Team, 2024) was used for data processing and model fitting.

RESULTS AND DISCUSSION

The average accuracy exhibited medium to high magnitudes, ranging from 0.43 to 0.98 for AUDPC L, from 0.80 to 0.97 for AUDPC M and from 0.73 to 0.97 for AUDPC U (Table 3).

Table 3. Results for individual analysis by location for the variables evaluated in eight soybean strains, assessed in Lavras, Ijaci, and Nazareno.

Area	FV	AUDPC L	AUDPC M	AUDPC U	AUDPC md	AUDPC oi	DESF	YIELD	Sowing Time
Ijaci	FG	11,86*	18.23*	19.65*	21.57*	3.40*	21,41*	28,37	Dec 12, 2020
	QME	393,61	2006,02	710,74	6368,00	10,93	54,44	42572,38	
	r$\hat{g}$g	0,96	0,97	0,97	0,98	0,84	0,98	0,98	
	Average	8,29	26,28	27,75	61,22	6,81	83,69	1840,14	
Lavras	FG	1.43*	18.23*	2.14*	1.65*	2,16*	4,94*	3.80*	Dec 11, 2020
	QME	145,37	979,26	95,06	446,08	2786.67	97,72	154490,81	
	r$\hat{g}$g	0,55	0,97	0,73	0,63	0,73	0,89	0,86	
	Average	10,61	34,12	6,54	25,68	83,85	88,13	2618,08	
Nazareno	FG	1.22*	0.57*	5.82*	4.32*	2.05*	15,33*	4,21	Dec 01, 2020
	QME	2,65	6341,24	1492,05	2388,57	12838,32	94,11	73661,46	
	r$\hat{g}$g	0,43	0,80	0,91	0,88	0,72	0,97	0,87	
	Average	0,70	86,74	73,25	108,28	922,53	78,07	1844,74	

FV: Source of variation; AUDPC L: Rust severity in the lower third; AUDPC M: Rust severity in the middle third; AUDPC U: Rust severity in the upper third; AUDPC md: Mean rust severity in the plot; AUDPC oi: Mean powdery mildew severity; DESF: Percentage of defoliation at the end cycle; YIELD: Yield (kg ha-1); Treatment calculated F-value and significance at 0,05 (FG); Residual mean square (QME); Accuracy (r$\hat{g}$g).

The accuracy, when considering the value of Fc (QMT/QME), accounts for the variation between cultivars, not just the experimental error, as represented by the coefficient of variation (CV). Thus, the higher the Fc value for the variation source of "Cultivars" is, the higher the accuracy and experimental precision associated with the observations. Notably, in all three environments, for all traits related to visual evaluation using a rating scale, significant differences were detected ($p < 0.05$) based on the F test.

Variance analysis allowed us to verify that there was no significant difference in the grain yield variable (YIELD), although disease occurrence negatively impacted the grain yield.

The average severity of Asian soybean rust (area under the disease progress curve (AACPD) md) and the average severity of powdery mildew (AACPD oi) differed among the Ijaci, Lavras and Nazareno environments. Notably, Nazareno exhibited a higher disease severity and a lower average yield than did the other environments.

These results emphasize the importance of the cultivation environment in the expression of these traits and suggest the presence of favorable conditions for disease development in Nazareno, leading to a crop yield reduction at that location. The higher mean Asian soybean rust and powdery mildew severity levels in Nazareno suggested greater disease pressure in that environment.

The rust severity frequency distribution (Figure 1) shows the difference between the cultivar treatments with INOX® technology and the susceptible control cultivar treatment for Asian soybean rust. Each class corresponds to the frequency of evaluation scores using the diagrammatic scale developed by Godoy, Koga and Canteri (2006).

The average susceptibility of the control cultivar (M6410 IPRO) to rust was lower than that of the INOX® cultivars, demonstrating that disease susceptibility negatively affects the productive

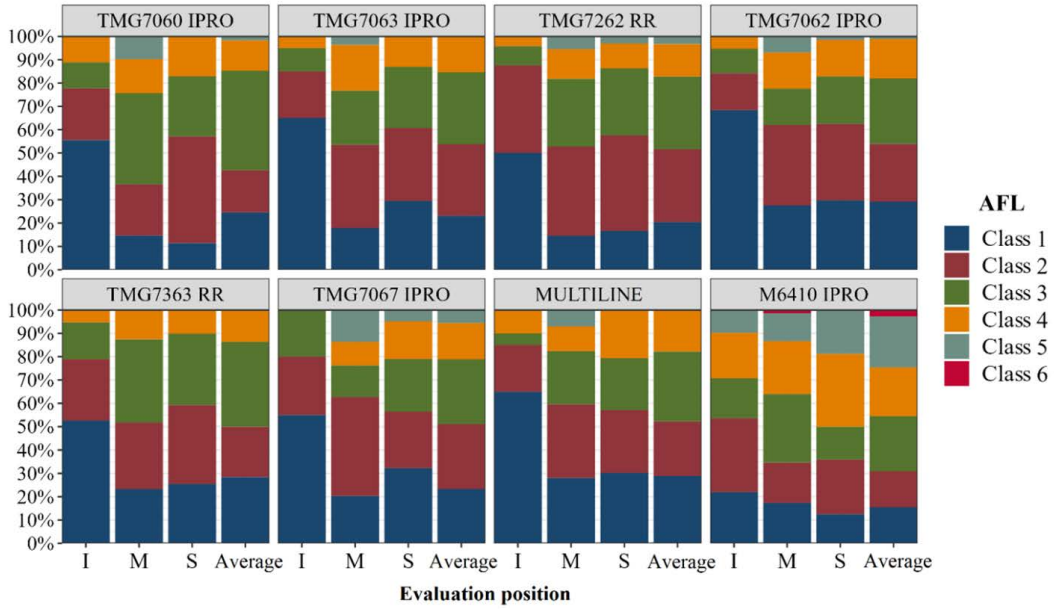

Figure 1. Frequency distribution of Asian rust severity, in percentage, based on the diagrammatic scale. AFL: Lesioned leaf area, I: Lower third; M: Middle third; S: Upper third.

performance of the genotype. A similar result was obtained by Geraldo and Adami (2020), whose cultivar TMG7062 IPRO showed lower severity than that of other susceptible cultivars, both in terms of management strategies with and without fungicide application during two harvests. Class 6, representing 78.5% of the Asian soybean rust severity, was observed only for the M6410 IPRO cultivar, while classes 5 (42% severity) and 4 (18% severity) exhibited greater magnitudes than those of the other genetic treatments.

Treatment with INOX® technology resulted in a greater proportion of class 1 (0.6% severity) in the lower third of the plants, indicating less disease progression. The presence of INOX® technology confers genes resistant to Asian soybean rust to the genotypes, resulting in reductions in symptoms, size and number of lesions and epidemic rate in the field compared to those of susceptible ones (Juliatti et al., 2019).

Compared with the susceptible cultivar M6410 IPRO, the genotypes with INOX® technology indicated lower progression of the average rust severity throughout the crop cycle at all plant positions (Figure 2). Partial resistance is characterized by reductions in the epidemic rate, number and size of lesions, and urediniospore production and an extended latent period. This causes reductions in the inoculum amount and disease intensity during the crop cycle (Juliatti et al., 2019).

Asian soybean rust is known to initially manifest in the lower parts of plants and later spreads to the upper parts. This pattern of ascending infection occurs for several reasons. The lower parts of soybean plants generally provide a more favorable environment for fungal development. The relative humidity is usually higher in the lower part of the plant due to less air movement and greater moisture retention in the lower foliage, providing the necessary conditions for spore germination and initial infection. The lower temperatures in the lower part of the plant are more conducive to fungal replication and pathogen development. The higher temperatures and sunlight exposure in the upper parts can limit fungal growth and dissemination (Juliatti; Pozza; Juliatti, 2021).

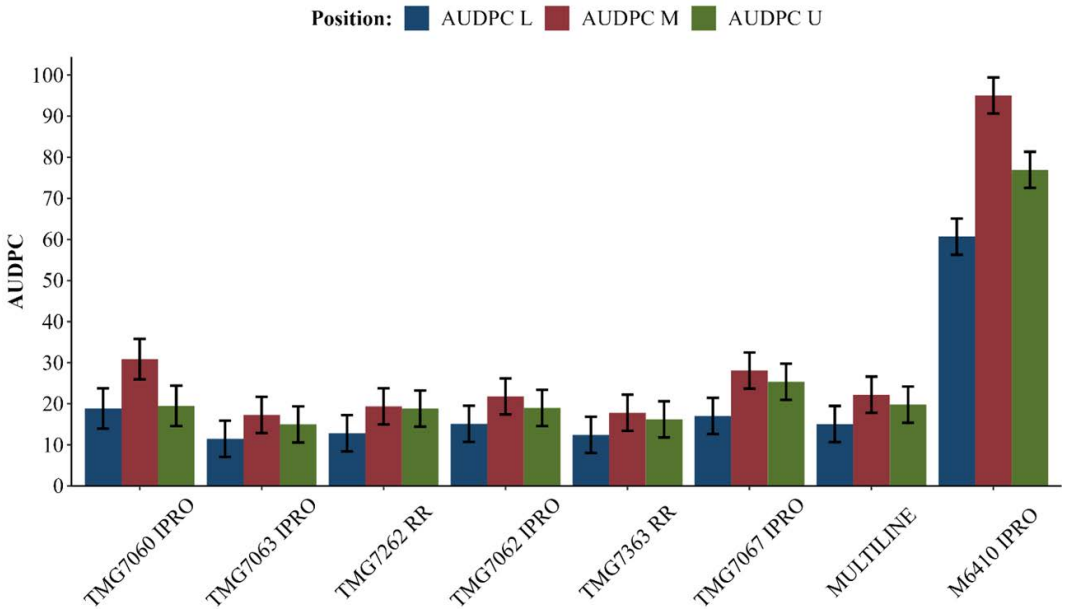

Figure 2. Results of Asian rust AUDPC aligned based on the position effect for the evaluated treatments. AUDPC L: Severity in the lower third; AUDPC M: Severity in the middle third; AUDPC U: Severity in the upper third.

As the infection develops in the lower part of the plant, the fungus continues to multiply and produce new spores. These spores are then carried by wind to the upper parts of the plant, where they encounter less favorable conditions, such as a higher temperature and lower relative humidity. However, even under these unfavorable conditions, the fungus can still infect plants, especially if there are prolonged periods of moisture or favorable weather conditions in the upper parts (Juliatti; Pozza; Juliatti, 2021).

According to Juliatti, Pozza and Juliatti (2021), no signs or symptoms of rust occurred at temperatures below 18°C or above 30°C, and the highest AUDPC values occurred at 24°C with a 24-hour leaf wetness period. In contrast, the lowest values were obtained at temperatures above 27°C.

The behavior of the multiline cultivar was similar to that of the cultivars with INOX® technology. This was expected based on the results obtained for the common bean crop. Mixtures comprising bean lines with different patterns of resistance to *Colletotrichum lindemuthianum* represent a suitable strategy to reduce anthracnose progression in the field and, consequently, reduce yield losses caused by this pathogen (Botelho et al., 2011).

According to Raboin et al. (2012), who investigated the use of mixtures with different proportions of susceptible cultivars against 100 isolates of *Magnaporthe oryzae*, the effectiveness of mixtures in reducing rice blast was demonstrated. Therefore, multiline cultivation is an appropriate strategy to increase phenotypic stability and reduce *Magnaporthe oryzae* progression in the field (Castro et al., 2022).

Notably, line mixing is an efficient strategy to increase phenotypic stability in soybean, while INOX® multiline cultivars are effective in reducing the severity of Asian soybean rust (Vilela et al., 2024).

The larger magnitude of AUDPC md in multienvironment analysis identifies this variable as a more comprehensive indicator of the average rust severity in the plot, encompassing relevant information on the disease as a whole. Therefore, only this variable was included in multienvironment analysis. Conducting multienvironment experiments to evaluate the agronomic performance of different genotypes is one of the basic objectives of plant breeding programs (Acquaah et al., 2016). One way to evaluate such experiments is by conducting a joint analysis across environments and cropping years (Ward et al., 2019).

In this study, the variation source of "Among Regular Cultivars (CR)" represents the treatments containing INOX® technology, while the variation source of "Among Lines (G)" represents the cultivars with INOX® technology, excluding the multiline cultivar. There was a combination of environmental oscillations inherent to the three considered environments (Ijaci, Lavras and Nazareno), as presented in the joint variance analysis summary (Table 4).

The environmental factors, such as soil fertility, represent predictable variations. However, the occurrence of rainfall and even high temperatures associated with the environment exhibit unpredictable variations, suggesting that they occur randomly. Therefore, the phenotypic contribution of the environmental component is due to the combination of predictable and unpredictable factors (Silva et al., 2017).

The above environmental effects were essential for the significant interaction of C × E for all evaluated traits according to the likelihood ratio test (LRT) (Table 4). Thus, these results emphasize the need to evaluate experiments in different environments (Soares et al., 2015). Notably, C × E interaction has been widely studied for soybean in Brazil and even in the present study region (Bianchi et al., 2022; Carvalho et al., 2023; Gesteira et al., 2018). The findings of this study corroborate previous findings and indicate that the behavior of the cultivars varied across the different environments.

Table 4. Results for the multi-environment analysis evaluated in eight soybean strains for Asian rust severity, powdery mildew severity, defoliation and yield.

FV	GL	N	AUDPC md	AUDPC oi	DESF	YIELD
Cultivars (C)	7	F	39854,20*	13531,29	1357,35*	61395,16
Among Regular C (CR)	6	F	6557,45*	4416,09	1321,65*	46916,69
Among Lineages (G)	5	F	6566,19*	7828,83	1507,93*	2711,70*
Mult vs G	1	F	37840,50*	11193,73	2875,33*	1829163,44*
Test vs G	1	F	264803,14*	11825,09	3529,35*	2013033,10*
Environment (E)	2	A	1436,93	256309,53*	19,38	195870,83*
Application (A)	3	F	8,05E+10	4,04E-05	6,79E+11	5,07E+07
C x A	21	F	26874,72*	1301,55	745,81*	701529,45*
C x E	14	A	2296,42*	257,47*	23,14*	41542,42*
A x E	6	A	92,61	7380,17*	8,71	486,54
Accuracy			0,98	0,49	0,97	0,86
QME			1946,16	10236,88	82,23	67447,82
Average			64,20	337,34	83,10	2098,05

FV: Source of variation; GL: Degrees of freedom; N: Nature of the effect (fixed or random); AUDPC md: Mean rust severity in the plot; AUDPC oi: Mean powdery mildew severity; DESF: Percentage of defoliation at the end cycle; YIELD: Yield in kg ha-1. *F-test for fixed effects (F) and Likelihood Ratio Test (LRT) for random effects (A) at a significance level of 0,05.

The quadratic component of the Cultivars (C) × Environment (E) interaction term was significant according to the LRT. Due to the influence of environmental factors on phenotypic expression, it is expected that there will be genotype × environment interactions, indicating that the behavior of different lines and/or cultivars will vary across the evaluated environments (Ramalho et al., 2012).

For defoliation (DESF) and AUDPC md, there was a significant effect for the quadratic components of Cultivars (C), the breakdown components of Among Regular Cultivars (CR) and Among Lines (G), the contrasts of Mult vs. G and Test vs. G, and the interaction term of Cultivars (C) × Applications (A) (Table 4).

The significant effect of the interaction of Cultivars (C) × Applications (A) indicates noncoincident behavior of the cultivars based on the number of fungicide applications for the grain yield, defoliation, and AUDPC md. The response to an increasing number of applications of fungicide FOX XPRO® was linear and positive for the grain yield. Similar results were obtained by Barros et al. (2008), Finoto et al. (2011), and Zambiazzi et al. (2018), where an increase in the number of applications led to an increase in the grain yield of 23%, 22%, and 28%, respectively.

An increase in the number of fungicide applications resulted in a decrease in the phenotypic means of both traits. Among the physiological effects of fungicides on crop metabolism, the inhibition of ethylene biosynthesis results in a greening effect, which delays senescence (Silva; Canteri; Silva, 2013). When analyzing the soybean cultivars, significant differences were observed in the mean values of AUDPC md among the cultivars. These differences indicate variations in disease susceptibility among the evaluated cultivars. These findings agree with the results of previous studies, indicating a positive genetic influence on soybean resistance to Asian soybean rust (Negrisoli et al., 2022).

The variable of AACPD oi exhibited a significant effect according to the LRT for the variance components of Environment (E), Cultivars (C) × Environment (E) interaction and Applications (A) × Environment (E) interaction. Similarly, the grain yield exhibited a significant effect according to the F test for the quadratic components of Among Lines (G) with INOX® technology and the contrasts of Mult vs. G and Test vs. G. The variance component of Environment (E), the interaction of Cultivars (C) × Applications (A) and the interaction of Cultivars (C) × Environment (E) were significant according to the LRT.

It has been reported that autogamous plant cultivars, due to possessing mostly homozygous loci, exhibit a lower individual buffering capacity, suggesting that they are more susceptible to biotic and abiotic stresses. Therefore, the choice of strategies for better adaptation to the effects of predictable and unpredictable environmental fluctuations requires careful selection of the genetic structure of populations (Bruzi; Ramalho; Abreu, 2007). An interesting strategy is genotypic mixing, which facilitates population homeostasis and, therefore, is more stable than pure lineage mixing (Carneiro et al., 2019).

During the final phase of the Asian soybean rust epidemic, lesions lead to leaf yellowing and subsequent senescence, which can even result in complete defoliation under severe infestations (Zambolim, 2019). In this study, AACPD md and DESF were negatively correlated (0.28) due to defoliation caused by the disease (Figure 3).

The correlation ($\rho = 0.61$) between the modified chlorophyll uptake ratio index (MPRI) and normalized difference vegetation index (NDVI) in this study ensures the possibility of using RGB

Figure 3. Pearson phenotypic correlations between the adjusted means for the studied variables.

*t-test at 0,2 significance level and ** at 0,05 significance level; NDVI: Normalized Difference Vegetation Index; AUDPC md: Mean rust severity in the plot; AUDPC oi: Mean powdery mildew severity; DESF: Percentage of defoliation at the end cycle; YIELD: Yield (kg ha-1).

and multispectral sensor images. In remote sensing applications, most current low-cost phenotyping approaches are based on the analysis of visible spectrum (RGB) images (Araus et al., 2018). Both vegetation indices showed a positive Pearson's correlation coefficient (MPRI = 0.76 and NDVI = 0.62) for the grain yield trait (YIELD) and significant effects according to the t test for the MPRI ($p < 0.05$) and NDVI ($p < 0.2$). Defining the correlation between vegetation indices and yield is relevant because in the presence of a correlation, it is possible to predict the yield in a simple, fast, inexpensive, and nondestructive way (Hoyos-Villegas; Fritschi, 2013).

Furthermore, the NDVI exhibited a notable negative correlation with leaf defoliation (-0.95) since this index is highly correlated with the chlorophyll content (Raddi et al., 2021) and the leaf area index (Liu et al., 2023). The MPRI also indicated a negative correlation with AACPD hi, with a significant effect ($p < 0.2$). The larger the average magnitude of the NDVI was, the lower the average leaf defoliation in the genetic treatments. The NDVI exhibited a significant effect according to the F test for the quadratic components of Cultivars (C), for the subdivisions of Among Regular Cultivars (CR) and Among Lineages (G), for the contrasts of Mult vs. G and Test vs. G, and for the interaction of Cultivars (C) × Measurements (M). The systematic error of Block × M was significant according to the LRT, indicating that the magnitude of the error varies among the measurements (Table 5).

The MPRI imposed a significant effect on the quadratic components of Cultivars (C), for the subdivisions of Among Regular Cultivars (CR) and Among Lineages (G), for the contrasts of Mult vs. G and Test vs. G, and for the interaction of Cultivars (C) × Measurements (M). The systematic errors of Block × M and Block × C were significant according to the LRT, indicating that the magnitude of these errors varies among the measurements. The accuracy for both indices was equal to 1. The CVe values were 5.26% for the NDVI and 28.56% for the MPRI.

Table 5. Results of the analysis of variance for the vegetation indices at different evaluation times.

FV	GL	N	NDVI	MPRI
Cultivars (C)	7	F	4,0276*	0,1570*
Among Regular C (CR)	6	F	4,1794*	0,1582*
Among Lineages (G)	5	F	4,0276*	0,1570*
Mult vs G	1	F	24,1617*	0,8155*
Test vs G	1	F	24,4032*	0,7806*
Measurement (M)	1/2	F	4,58E-03	4,00E-05
C x M	7/14	F	0,2077*	0,0095*
Block x M	35/70	A	0,0051*	0,0015*
Block x C	245	A	0,0002	0,0006*
Accuracy			1	1
QME			0,00198	0,0004
CVe			5,26	28,56
Average			0,6308	0,1277

FV: Source of variation; GL: Degrees of freedom; N: Nature of the effect (fixed or random); NDVI: Normalized Difference Vegetation Index; MPRI: Modified Photochemical Reflectance Index.

*F-test for fixed effects (F) and LRT (Likelihood Ratio Test) for random effects (A) at a significance level of 0,05.

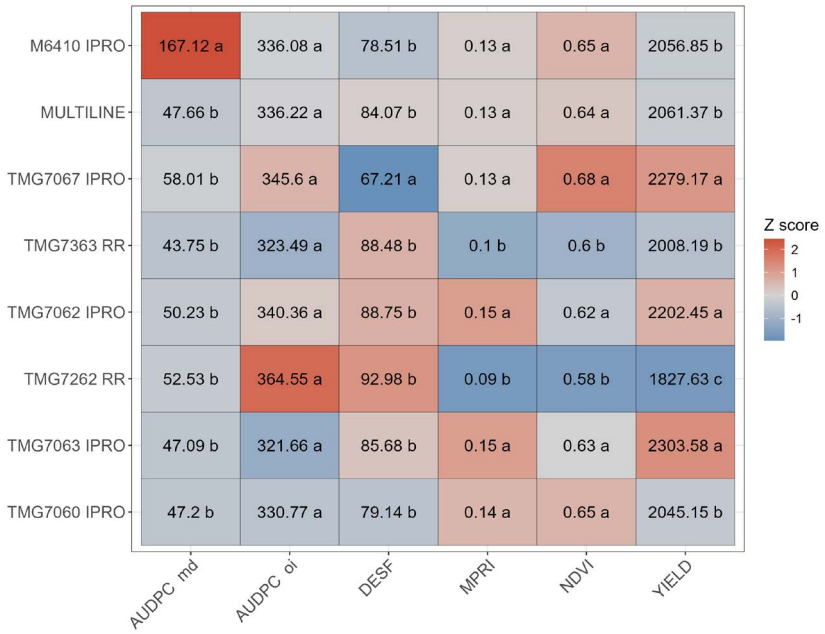

Figure 4. Scott-Knott comparison test for the analyzed variables ($p < 0.05$). Means followed by the same letter in the column do not differ statistically from each other. The colors represent the magnitude of the adjusted means on a normalized scale.

For the NDVI, the magnitude of the multiline average was very close to the average for the INOX® cultivars. However, the same did not occur for the MPRI (Figure 4). Although the genotypes are similar, there are genetic differences between the evaluated cultivars due to their different genetic origins, which, combined with environmental factors, results in differences in phenotypic observations (Gesteira et al., 2018). Vegetation indices calculated from red and green reflectance values are correlated with the composition of the pigment pool, specifically the chlorophyll/carotenoid ratio, which is sensitive to the dynamics of vegetation photosynthesis (Li et al., 2023).

The results demonstrated a correlation between the MPRI, AACPD and yield grain at the R5.5 phenological stage. This confirms the possibility of estimating the disease severity and damage levels through RGB images, rendering it an important experimental tool with a low cost, thus potentially reducing the need for visual and subjective assessments of the disease severity (Franchini et al., 2018). Furthermore, these results suggest that soybean cultivars respond differently to fungicide applications. The variations in the responses of the evaluated indices and the yield grain could be attributed to differences in the physiological and genetic characteristics of the cultivars, as well as to the interactions between genetic and environmental factors.

UAVs are technologically advanced, highly efficient, low-cost systems that can perform actions in real time and support precision agriculture to increase production with lower environmental risks. Over the last decade, UAV-based aerial images have provided new perspectives on the production environment, supporting decision-making regarding management practices (Istiak et al., 2023)

Therefore, vegetation indices provide information for various precision agriculture practices, offering quantitative data on crop growth and health (Radocaj et al., 2023) and facilitating nondestructive, remote and real-time monitoring. These indices are emerging as important tools for use in plant breeding programs as alternatives for high-throughput phenotyping efforts. By leveraging UAV technology and vegetation indices, researchers and farmers can gain valuable information on the performance and health of soybean crops. This information can support decision-making processes, optimize resource allocation and contribute to more efficient and sustainable soy production (Crusiol et al., 2024).

Overall, the integration of aerial imagery, high-throughput phenotyping, and genotypic information into soybean genetic improvement programs can enhance the efficiency and effectiveness of genetic improvement efforts. These technologies provide valuable information on the crop performance, assist in the selection of superior genotypes and contribute to sustainable agricultural practices. Continuous research and application of these tools are crucial to advancing soybean genetic improvement and achieving greater yield and profitability levels in soybean production systems.

The vegetation indices NDVI and MPRI were highly correlated, supporting the use of RGB and multispectral sensors for high-throughput phenotyping in assessments of the grain yield and severity of Asian soybean rust and powdery mildew in soybean crops in high-altitude tropical climates. High-throughput phenotyping facilitates the more accurate evaluation of the grain yield and severity of Asian soybean rust and powdery mildew in soybean crops. This information is essential for making informed decisions regarding crop management strategies, disease control measures and productivity optimization in legume cultivation in high-altitude tropical regions.

The correlation between the percentage of defoliation and NDVI demonstrates how this index can be applied in genetic improvement programs aimed at obtaining cultivars resistant to disease. In addition, the severity of Asian soybean rust under tropical conditions was quantified. The

absence of a significant relationship between the severity of Asian soybean rust and the evaluated traits suggests that other factors, such as genetic resistance or environmental conditions, may more notably influence the development and severity of Asian soybean rust.

ACKNOWLEDGMENTS

The authors are especially grateful to the National Council for Scientific and Technological Development (Conselho Nacional de Desenvolvimento Científico e Tecnológico - CNPq) and the Minas Gerais State Agency for Research and Development (Fundação de Amparo à Pesquisa do Estado de Minas Gerais - FAPEMIG) for their support, as well as the Brazilian Federal Agency for Support and Evaluation of Graduate Education (Coordenação de Aperfeiçoamento de Pessoal de Nível Superior - CAPES) for the scholarships granted and also for the research productivity scholarship. We would like to thank the CNPq also for the research productivity fellowship granted to the coauthor Dr. Adriano Teodoro Bruzi and the Federal University of Lavras (UFLA) for all its support of this research.

DISCLOSURE STATEMENT

No potential conflict of interest was reported by the author(s).

REFERENCES

Abbas A, Zhang Z, Zheng H, Alami MM, et al. (2023). Drones in Plant Disease Assessment, Efficient Monitoring, and Detection: a way forward to smart agriculture. *Agronomy*. 13: 1524.

Acquaah G, Al-Khayri JM, Jain SM, Johnson DV. (2016). Conventional Plant Breeding Principles and Techniques. *Advances in Plant Breeding Strategies: Breeding, Biotechnology and Molecular Tools.* p.115-158.

Alves KS, Guimarães M, Ascari JP, Queiroz MF, et al. (2021). RGB-based phenotyping of foliar disease severity under controlled conditions. *Tropical Plant Pathology.* 47: 105-117.

Barros HB, Sediyama T, Silva Reis M, Cecon PR. (2008). Efeito do número de aplicações de fungicidas no controle da ferrugem asiática da soja. *Acta Scientiarum. Agronomy.* 30: 2.

Bevers N, Sikora EJ, Hardy NB. (2022). Soybean disease identification using original field images and transfer learning with convolutional neural networks. *Computers And Electronics In Agriculture.* 203: 107449.

Botelho FBS, Ramalho MAP, Abreu ADFB, Rosa HJA. (2011). Multiline as a Strategy to Reduce Damage Caused by Colletotrichum lindemuthianum in Common Bean. (Report). *Journal of Phytopathology*. 159: 175.

Crusiol LGT, Sibaldelli RNR, Nanni MR, Franchini JC, Farias J R B. Conceitos e definições de sensoriamento remoto para monitoramento da soja. Londrina: Embrapa Soja.

Ferraz MAJ, Barboza TOC, Arantes PdeS, Von Pinho RG, et al. (2024). Integrating Satellite and UAV Technologies for Maize Plant Height Estimation Using Advanced Machine Learning. *Agriengineering.* 6: 20-33.

Finoto EL, Carrega WC, Sediyama T, Albuquerque JAA, et al. (2011). Efeito da aplicação de fungicida sobre caracteres agronômicos e severidade das doenças de final de ciclo na cultura da soja. *Revista Agroambiente.* 5: 44-49.

Franchini JC, Balbinot Junior AA, Jorge LAdeC, Debiasi H, et al. (2018). Uso de imagens aéreas obtidas com drones em sistemas de produção de soja. Londrina: Embrapa Soja.

Gesteira GDS, Bruzi AT, Zito RK, Fronza V, et al. (2018). Selection of early soybean inbred lines using multiple indices. *Crop Science.* 58: 2494-2502.

Godoy CV, Koga LJ, Canteri MG. (2006). Diagrammatic scale for assessment of soybean rust severity. *Fitopatologia Brasileira.* 31: 63-68.

Istiak MA, Syeed MMM, Hossain MS, Uddin MF, et al. (2023). Adoption of Unmanned Aerial Vehicle (UAV) imagery in agricultural management: a systematic literature review. *Ecological Informatics.* 78: 102305.

Juliatti FC, Mesquita ACO, Teixeira FG, Beloti IF, et al. (2019). Characterization of soybean genotypes showing partial resistance to soybean rust. *Summa Phytopathologica.* 45: 313-319.

Juliatti BCM, Pozza EA, Juliatti FC. (2021). Research Article Severity of rust infection in soybean genotypes with partial resistance as a function of temperature and leaf wetness duration. *Genetics And Molecular Research.* 20: 2.

Li W, Chen R, Ma D, Wang C, et al. (2023). Tracking autumn photosynthetic phenology on Tibetan plateau grassland with the green–red vegetation index. *Agricultural And Forest Meteorology.* 339: 109573.

Liu Y, An L, Wang N, Tang W, et al. (2023). Leaf area index estimation under wheat powdery mildew stress by integrating UAV-based spectral, textural and structural features. *Computers And Electronics In Agriculture.* 213: 108169.

Raboin LM, Ramanantsoanirina A, Dusserre J, Razasolofonanahary F, et al. (2012). Two-component cultivar mixtures reduce rice blast epidemics in an upland agrosystem. *Plant Pathology.* 61: 1103-1111.

Raddi S, Giannetti F, Martini S, Farinella F, et al. (2021). Monitoring drought response and chlorophyll content in Quercus by consumer-grade, near-infrared (NIR) camera: a comparison with reflectance spectroscopy. *New Forests.* 53: 241-265.

Radocaj D, Siljeg A, Marinovic R, Jurilic M. (2023). State of Major Vegetation Indices in Precision Agriculture Studies Indexed in Web of Science: a review. *Agriculture.* 13: 707

Resende MDVde, Silva FFe, Azevedo CF. (2014). Estatística matemática, biométrica e computacional: modelos mistos, multivariados, categóricos e generalizados (REML/BLUP), inferência bayesiana, regressão aleatória, seleção genômica, QTL-GWAS, estatística espacial e temporal, competição, sobrevivência. Viçosa: Suprema.

Shahi TB, Xu CY, Neupane A, Guo W. (2023). Recent Advances in Crop Disease Detection Using UAV and Deep Learning Techniques. *Remote Sensing.* 15: 2450.

Shammi SA, Huang Y, Feng G, Tewolde H, et al. (2024). Application of UAV Multispectral Imaging to Monitor Soybean Growth with Yield Prediction through Machine Learning. *Agronomy.* 14: 672.

Silva EEda; Baio FHR, Teodoro LPR, Silva Junior Cada, et al. (2020). UAV-multispectral and vegetation indices in soybean grain yield prediction based on in situ observation. *Remote Sensing Applications: Society and Environment.* 18: 100318.

Silva KB, Bruzi AT, Zambiazzi EV, Soares IO, et al. (2017). Adaptability and stability of soybean cultivars for grain yield and seed quality. *Genetics and Molecular Research.* 16: 1-15.

Soares IO, Rezende PMD, Bruzi AT, Zambiazzi EV, et al. (2015). Adaptability of soybean cultivars in different crop years. *Genetics and Molecular Research.* 14: 8995-9003.

Vilela NJD, Carvalho ACHF, Bruzi AT, Medeiros FCL, et al. (2024). Multiline is a strategy for homeostasis and Asian Soybean Rust Management in Agriculture. *Genetics And Molecular Research.*

Ward BP, Guedira GB, Tyagi P, Kolb FL, et al. (2019). Multienvironment and multitrait genomic selection models in unbalanced early-generation wheat yield trials. *Crop Science.* 59: 491-507.

Yang Z, Willis P, Mueller R. (2008). Impact of Band-Ratio Enhanced AWIFS Image to Crop Classification Accuracy. In: Pecora – The Future of Land Imaging… Going Operational, 17. 2008, Denver, Colorado, USA. **Proceedings...** Maryland: (ASPRS.

Zambiazzi EV, Bruzi AT, Zuffo AM, Soares IO, et al. (2018). Effects and management of foliar fungicide application on physiological and agronomical traits of soybean. *Australian Journal of Crop Science.* 12: 265.

Zambolim L, Mochko ACR, Parreira DF, Valadares SV. (2019). Potassium Fertilization Reduces the Severity of Asian Soybean Rust Under High Disease Pressure. *Journal Of Agricultural Science*. 11: 116.

Zhao H, Yang C, Guo W, Zhang L, et al. (2020). Automatic Estimation of Crop Disease Severity Levels Based on Vegetation Index Normalization. *Remote Sensing.* 12: 1930.

Supplemetary Figures

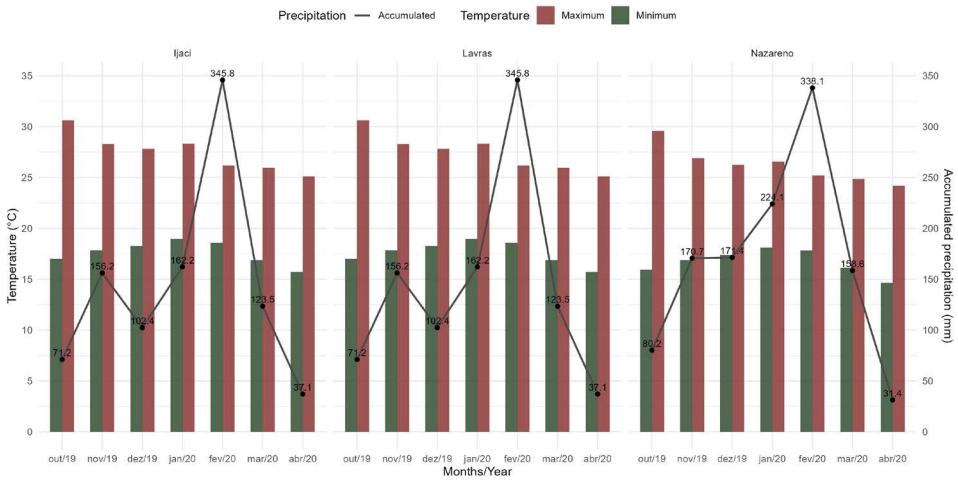

Figure S1. Accumulated precipitation, maximum and minimum temperatures from october to april in (a) Ijaci, (b) Lavras and (c) Nazareno, Minas Gerais.

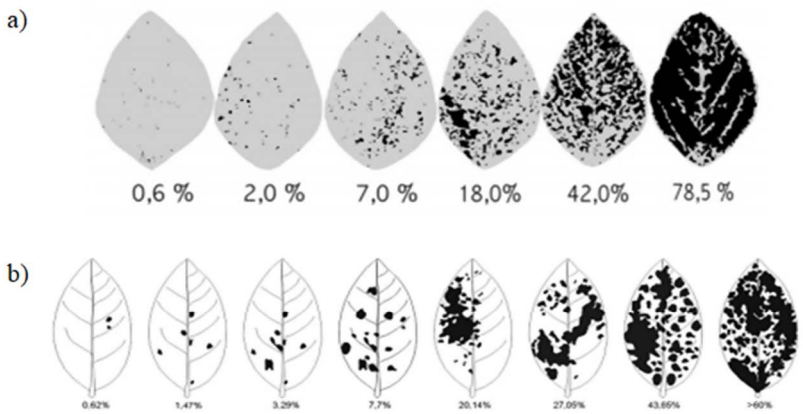

Figure S2. Diagrammatic scale for assessment of (a) asian soybean rust (Phakopsora pachyrhizi) severity and (b) powdery mildew (Erysiphe difusa) in soybean crops.

Table S1. Description of the cultivars, maturity groups (MG), and tecnology.

Origin	MG	Tecnology
TMG 7060 IPRO	6.0	INTACTA RR2 IPRO/ INOX®
TMG 7063 IPRO	6.3	INTACTA RR2 IPRO/ INOX®
TMG 7262 RR	6.2	RR/ INOX®
TMG 7062 IPRO	6.2	INTACTA RR2 IPRO/ INOX®
TMG 7363 RR	6.3	RR/ INOX® / Resistente à Cisto
TMG 7067 IPRO	6.7	INTACTA RR2 IPRO/ INOX®
MULTILINHAS	-	-
M 6410 IPRO	6.4	INTACTA RR2 IPRO®